Soft tissue strain rates in side-blast incidents

Bastien, H.[1], Bouamoul, A.[2], Rancourt, D.[1]

[1]Groupe de recherche PERSEUS, Université de Sherbrooke, 2500, boul. de l'Université, Sherbrooke, QC, Canada, J1K2R1 (hugo.bastien@creaform3d.com)
[2] Defence Research and Development Canada – Valcartier, 2459 Route de la Bravoure, Québec, Qc, Canada, G3J 1X5

Abstract. Complexity of injury mechanisms in blast-like events requires constant evolution of vulnerability modelling for improving the prediction of trauma consequences, and for the establishment of mitigating strategies. Refinement of numerical techniques, along with appropriate material characterization, leads to improved fidelity and accuracy with regards to injury assessment. However, the accuracy of numerical models strongly relies on test data, specifically mechanical properties of anatomical structures. Testing conditions that are representative of side-blast incidents are still to be evaluated in order to improve models' representativeness. This paper introduces a simplified finite element model of a human neck to study the reaction of armour vehicle occupants exposed to side-blast incidents. The model was used to identify which anatomical structures may suffer injury and the strain rates that neck tissues may experience. Based upon DRDC Valcartier results using a vertical drop tower to approximate global acceleration induced by blast-like incidents, a velocity–time curve was used as boundary conditions on the torso kinematics. Head and vertebrae were modelled as rigid bodies with proper muscle and ligament attachments. Nuchal and anterior longitudinal ligaments were included because of their role in stabilizing body joints subjected to excessive motion. Seven muscle groups were modelled. The muscle models included fasciae to investigate whether they may play a significant role in restraining neck motion. Simulation results showed that the anterior longitudinal ligament strain reached a maximum of 20% in the C7-T1 portion and up to 100 % at the C0-C1 level due to head hyper-extension. The soft connective tissues experienced important strain rate magnitude on the order of 200 s^{-1} in the upper C0-C1 portion of the anterior longitudinal ligament. Therefore, future anatomical FE models in side blast incidents should consider soft tissue properties at strain rates up to 300 s^{-1} to account for variations in soft tissue constituents.

Keywords: side blast, neck model, connective tissue injury, neck fasciae, soft tissue strain rate

1. INTRODUCTION

Injury criteria are often needed as design specifications for various devices that physically interact with humans, particularly for those which protect individuals in falls, vehicle crashes or mine blasts as for light armour vehicles (LAV). The establishment of meaningful injury criteria is, however, a challenging task that is still under extensive studies.

In the 1950's-60's, it was acknowledged that both acceleration levels and duration of impacts had to be considered when determining safety thresholds. Both Eiband (1959) [1] and Huculak (1990) [2] wrote excellent reviews on the subject, providing data that clearly demonstrate that higher acceleration levels are possible (80 to 100-G) when pulse durations are shorter (about 20 ms). A number of authors (Stapp 1961 [3]; Zaborowski 1965 [4]) further pointed out the need to vary threshold levels depending on the direction of the acceleration vector relative to the body. In his review, Eiband [1] did warn readers that global acceleration limits can hardly be extended to all situations because seat impedance and means to strap subjects to a seat may significantly change how the body react to the platform/vehicle global acceleration level and, therefore, the resulting potential injury. Given this uncertainty and variability in acceleration levels during impacts, a conservative approach was followed and injury criteria were set in terms of seat/platform acceleration limits: 14.5-G for helicopter seat applications (Desjardins and Harrison 1972 [5]) or 20-G for seat ejection systems (Eiband 1959). Such low acceleration threshold, however, is irrelevant in many impact situations where acceleration levels may exceed 20-G.

Less conservative criteria were then proposed. Regarding head injuries, the head average change of momentum over a given time period was investigated, leading to criteria such as the GSI (i.e. Gadd Severity Index; Gadd 1962 [6]) or the HIC (i.e. Head Injury Criterion; Lowenhielm 1975 [7]). Later on, Newman (1986) [8] introduced a new criterion called the Generalized Acceleration Model for Brain Injury (GAMBIT) that incorporates both linear and angular accelerations in the prediction of head injury. More recently, Newman *et* al. (2000) [9] proposed a Head Impact Power (HIP) injury

assessment function that relies essentially on the rate of change of the head kinetic energy, including both linear and angular contributions in the computation. Chest injuries were also considered and led to either the Combined Thorax Index (CTI) or the Trauma Thorax Index (TTI) (Digges 1998 [10]). Chest contact forces were also proposed as injury criteria by Viano (1984) [11] and Eppinger (1976) [12]. Two decades ago, Lau and Viano (1986) [13] studied the validity of combining both compression and chest compression rate into a single criterion named the VC criterion. That criterion is of particular interest because it differentiates the resulting injury depending on the relative amplitude of compression vs. compression rate and it includes tissue strain rate in the analysis, a novel approach at that time.

The abovementioned criteria, however, all share the same weakness. The injury criteria were determined by correlating criteria values to known injury databases or cadaver studies such as those conducted to obtain the Wayne State Tolerance Curve (Lissner et al. 1960 [14]). Hence, their application is limited to the specific impact conditions of reference. Knowledge acquired from these specific tests is unfortunately not easily transferable to other impact situations.

Aware of these limitations, a number of investigators instead proposed criteria that are associated with internal body stresses or strains/displacements. For instance, limits on loads were proposed at various critical locations in the body, including the neck (King et al. 1981 [15]; Digges 1998), the spine (Stech and Payne 1969 [16]; Shane 1985 [17]; Coltman 1983 [18]; Chandler 1985 [19]), the chest (Viano, 1984; Eppinger 1976) or for the femur (10 kN upon Digges 1998). Brain motion was recently investigated by King *et* al (2011) [20] while tissue strain was considered early by Stalnaker *et* al. (1971) [21] as the Mean Strain Criteria (cited in Hannon 2006 [22]). Criteria based on internal stresses or strains however, strongly rely on the availability of accurate models of the human body to estimate those variables in various impact conditions.

A number of human body models and anthropomorphic test devices (ATD) models already exist in the field of crashworthiness. Examples of available human models used in the past are the GEBOD (Cheng *et* al. 1994 [23]; Lockhart 2010 [24]), the ATB (Cheng *et* al. 1998 [25]) and various ATD models: Madymo and FTSS Hybrid III models. These models compute segment kinematics and joint interacting forces during and following impact. Ultimately, injury criteria should be based on tissue states/strain rates and precise tissue lesions of the anatomical structures, data that cannot be obtained from the abovementioned models.

Anatomical models are required for that purpose, along with knowledge of tissue mechanical properties (Sligtenhorst et al. 2006 [26]) and material failure. Anatomical models have greatly improved over the last few years, thanks in part to the recent developments in imaging technologies. But determination of tissue mechanical properties and associated material failure limits remain, from our point of view, the main challenging issues. For instance, a whole body of literature already exists on mechanical properties of biological tissues at low strain rate, but much less at higher values. Sligtenhorst *et* al. (2006) recently reported bovine muscle tissue compressive response for strain rates of 1000 s-1 to 2500 s-1 for a 80% strain, while Song *et* al. (2007) [27] succeeded to measure porcine muscle tissue mechanical properties at up to 3650 s-1 for a 45% strain. These tests were performed with split Hopkinson bars while McElhaney (1966) [28] tested bovine muscle tissue using a compression impact gas-gun at strain rates ranging from 0.001 s-1 to 1000 s-1.

The use of tissue mechanical properties data from the abovementioned studies, for impacts situations, is however questionable for many reasons. Firstly, tissue preparations were taken at different time periods that are relative long post-mortem and tissue microstructure may have changed upon preservation protocols. Secondly, tests were conducted on bovine tissue muscle in compression while, in many instance, soft tissues are subjected to tension. Thirdly, bovine muscle tissue does include connective tissues but with a lesser content than connective tissue anatomical structures that are highly involved in body injuries due to high acceleration initial conditions namely, tendons, ligaments and fasciae. Finally, except for McElhaney's data [28], strain rates measured may greatly exceed those encountered in impact scenarios. Zhang *et* al (2008) [29] suggested that blasts events should be in the range of 1000 to 3000 s-1 while strain rates are reported to be in the range of 1 s-1 for motor vehicle crashes or falls. Therefore, there is no consensus on what strain rate should be used to elaborate accurate human body models under various impact situations.

As a first approximation, one could simply extrapolate data from the abovementioned studies, at representative strain rates of the impact scenario under study, assuming no significant variation in mechanical properties with strain rate. From our point of view, this approach is not conservative. As a matter of fact, literature suggests that soft tissues are polymer gels that exhibit phase transitions (e.g. Tanaka 1992 [30]). Hence, they show a strong discontinuity in their physical properties at their glass transition temperature T_g. Data from the literature indicate that connective soft tissue T_g is in the order of -1 ^{o}C for rat tail tendon native collagen fibers (Fathima *et* al. 2010 [31]), down to -10 ^{o}C for bovine

tendon fascicle (Tzou *et* al. 1997 [32]), and between -5 to -1 ^{o}C for cornea (Seiler *et* al. 1983 [33]). Therefore, based on the time-superposition principle (Lillie and Gosline 2002 [34]), if soft tissues are exposed to sufficiently high strain rates during impacts or blasts, they may bring their Tg at about body temperature. As a result, soft tissues would behave as a brittle material with very high static stiffness during impact. As an example, pure elastin, one of the main components of soft tissues, when changing from a rubbery to a glassy state, sees its tangent modulus change by a factor of 262 (Lillie and Gosline 2002). Unfortunately, we do not yet know whether connective tissues Tg can be raised up to body temperature for strain rates in the range of those encountered in body impacts or mine blasts. If so, current mechanical models of human body impacts may not be conservative and tissue failure may occur much earlier than expected.

Obviously, there is a need to develop mechanical models of the human body that incorporate accurate tissue material properties that span the whole possible range of strain rates encountered during impacts or blasts. Given the technical complexity of developing systems that can measure valid tissue properties over high strain rates, while maintaining viability of tissue cells, it is advisable to first estimate the strain rate range than can be encountered in strenuous impact conditions such as mine blasts. This constitutes the specific purpose of the present paper. A finite element anatomical model of the neck and head was thus developed to estimate the maximum strain rate observed within the main anatomical structures when a seated individual was subjected to a mine blast event. We focused on the neck because it is known to be one of the sites of injuries during blasts (Ramasamy *et* al. 2008 [35]) and most likely, a region where high strain rates should be observed.

2. METHODOLOGY

A finite element (FE) model of a human body seated laterally in a LAV was developed using LS-Dyna Hydrocode. Overall FE model included 797836 nodes and 697874 elements. Given that we focused our study on the neck region, we assumed a rigid torso (3680 rigid elements) and we modelled relevant anatomical structures that restrain head motion: vertebrae (37744 rigid elements), the nuchal fasciae or ligament (12690 tension-only membrane elements), the neck muscles (454934 hexahedral elements), muscle fasciae (178056 tension-only membrane elements) and the anterior ligament (532 tension-only membrane elements). We did not use existing mannequin FE models since, although they provide rigid body kinematics and joint forces and moments, they provide no information on the loading of the detailed anatomical structures. Such information is important because protective headgears should primarily target the critical anatomical structures that may be first injured. Neck models of various complexities have been developed previously (Linder 2000 [36]; Küçük 2007 [37]; Jiango *et* a. 2007 [38]; Bourdet and Willinger 2008 [39]), but these models show important limitations regarding damages sustained by soft tissues. Soft tissues (muscles and ligaments) are sometimes modelled with 1D-elements (Wittek *et* al. 2001 [40]; Van Lopik and Acar 2004 [41]; Teo 2007 [42]; Panzer 2011 [43]) to include their influence on head motion. However, since soft tissues are not explicitly represented, their internal stress and strain evaluation is limited.

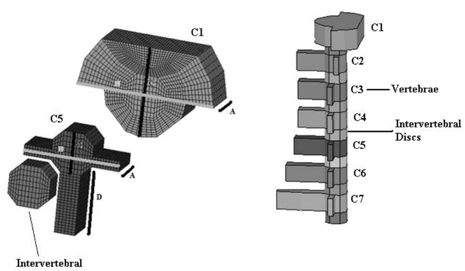

Figure 1: Geometry of Vertebrae and IV Discs as used in the neck model.

Head and vertebrae were modelled as rigid bodies and their dimensions were adjusted to accurately locate muscles and ligaments attachments according to McMinn *et* al. (1993) [44] as shown in Figure 1 and Table 1. Vertebrae densities were adjusted individually to simulate individual vertebrae masses (Stemper et al. 2006) [45]. Inter-Vertebral (IV) discs were modelled with 3D elements (6944 hexahedral elements) that can predict the shear stress experienced by each disc. The IV discs'

mechanical properties were adjusted to approach the stiffnesses reported by Küçük (2007) given in Table 2. A torsion spring element was located at joint C0-C1 while joint C1-C2 had to be stiffened slightly more to avoid numerical instabilities. Ligaments were also included in the numerical model because of their stabilizing role in the joint articulations during large joint motions. Both the nuchal and the anterior longitudinal ligaments were modelled using shell elements (assuming a uniform thickness of 2 mm) to study the stress and strain distribution. The ligament material properties were adjusted using data from Stemper *et* al. (2006), with a Young modulus of 19 MPa.

Table 1: Vertebrae dimensions as used in the finite element model (upon McMinn (1993)).

Vertebra	A (mm)	B (mm)	C (mm)	D (mm)
C1	-	-	47.6	-
C2	-	-	14.2	20.9
C3	13.5	16.9	14.2	18.8
C4	12.6	17.8	14.8	19.3
C5	12.2	19.0	15.2	22.4
C6	12.0	20.9	15.6	27.7
C7	13.0	24.6	15.5	34.9

Table 2: Intervertebral segment stiffness (upon Küçük (2007)).

Joint	Rigidity (Nm/deg)
C0-C1	0.02
C1-C2	0.06
C2-C3	10.22
C3-C4	11.92
C4-C5	12.33
C5-C6	13.37
C6-C7	14.11

Seven important muscles groups were modelled. They are the trapezius, the levator scapulae, the longissimus, the longus, the scalenus, the splenius capitis and the sternocleidomastoid. These seven groups were considered because they are known to play a significant role in controlling head motion during impacts (Conley *et* al. 1997) [46]. Each muscle core was modelled using 3D elements and a linear isotropic constitutive model with a Young modulus of 11 MPa (data extrapolated from McElhaney 1966), and the bulk material was surrounded by a connective tissue envelope modelled with shell elements that have different mechanical properties. Since fascia mechanical properties are not well documented, a sensitivity analysis was performed in the numerical simulations varying fascia stiffness to evaluate its impact on the results. Kureshi *et* al. (2008) [47] measured transversalis fascia Young modulus between 0.4 MPa and 10 MPa. The Zeng *et* al. (2003) [48] study on nasal fascia showed a modulus around 6 MPa. Since these two studies were performed at very low strain rate and since an increase of strain rate is known to cause the stiffening of soft connective tissues (Haut and Haut 1997 [49]; Panjabi *et* al. 1998 [50]; Crisco *et* al. 2002 [51]; Koh *et* al. 2004 [52]; Ng *et* al. 2004 [53]; Sligtenshorst *et* al. 2006; Song *et* al. 2007) a nominal Young modulus of 22 MPa was used across the model. This simplified fascia-bulk material model of a muscle, inspired from the work of Hukins *et* al. 1990 [54]), is unusual but it provides, from our point of view, a much better muscle model approximation than a simple 1D element. The cross-sectional area for each muscle was based on MRI measurements on 20 active students (Conley *et* al. 1997) and muscular density was set to 1.112 g/cm^3 (Ward and Lieber 2005 [55]). Table 3 summarizes the origin, insertion and cross-section areas used in each muscle model. Notice that muscles were considered as passive components, with no reflex loop, since typical blast duration are well under reflex response times; reflex contraction does not initiate in sufficient time to mitigate whiplash injuries and do not alter spinal kinematics (Stemper 2006). The level of muscle contraction was indirectly studied by performing a sensitivity analysis on muscle properties.

Table 3: Characteristics of muscle groups selected in the FEM (upon Conley *et* al. (1997))

Muscles	CSA (mm^2)	Origins	Insertions
Trapezius	150	Occipital bone Nuchal Ligament C7-T12	Shoulder
Levator Scapulae	150	C1-C4	Scapula
Longissimus	130	Thoracic Vertebrae	Mastoid
Scalenus	180	C2-C6	1st rib
Sternocleidomastoid	380	Clavicle	Mastoid
Longus	120	Occipital bone	Thoracic Vertebrae
Splenius Capitis	300	C7-T6	Mastoid

Although the overall model was three-dimensional in nature, the input to the model was a planar motion of muscle and ligament attachments at the torso level. The prescribed motion was obtained in two phases. The first phase consisted in performing real side blast tests on a vehicle and measuring typical velocity profiles of a seat where potential occupants could be seated. In the second phase, this velocity profile was then reproduced using a vertical drop tower testing facility developed by Defence Research and Development Canada (DRDC) Valcartier, to determine, this time, a velocity profile (see Figure 2) of a Hybrid III mannequin torso during drop and subsequent impacts. All material properties were assumed to be linear as a first approximation. Computer simulations were performed with LS-DYNA 971 software on MAMMOUTH-SERIE II (A super-computer of the Réseau Québécois de Calcul de Haute Performance, with a peak compute performance of 27 596 GFlops).

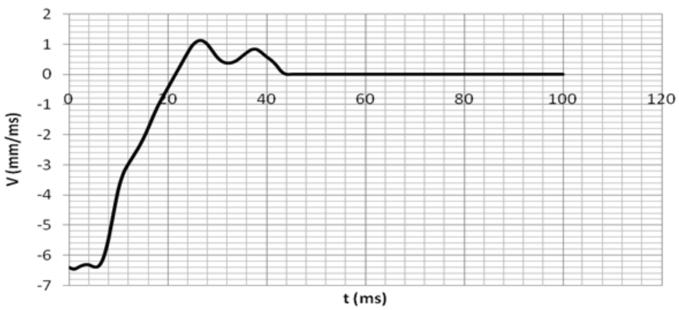

Figure 2: Torso motion imposed in the model.

3. RESULTS

Simulation results show that the anterior longitudinal ligament strain reaches a maximum of 20% in the C7-T1 portion and up to 100% at the C0-C1 level, causing an excessive hourglass of the elements which in turn led to error termination. There are two instances when the anterior longitudinal ligament reaches a peak of deformation. Firstly, it occurs when the head reaches its maximal backward position (at ~30ms, Figure 3). At that moment, the lower neck experiences tension and the lower portion of the anterior longitudinal ligament (between C7-T1) is maximally deformed (18%) and the upper portion (C0-C1) does not experience any tension (upper neck flexion). Secondly, after reaching that position, the head bounces forward (Figure 3) and the upper neck experiences a hyper-flexion until the strain in the C0-C1 anterior longitudinal ligament portion becomes excessive, leading to premature termination of the simulation. The nuchal ligament strain reaches 35% while the head bounces forward and its recoil is the cause of the anterior longitudinal ligament high deformation in the upper (C0-C1) portion (Figure 4). The nuchal ligament reaches a maximal deformation at the same time (~30ms) as the anterior longitudinal ligament lower (C7-T1) portion. The nuchal ligament experiences its 35% maximal strain locally near C1 while the trapezius and sternocleidomastoid fasciae experience a maximal deformation limited to 14% (Figure 6). A sensitivity analysis of the ligaments and muscle fascia mechanical properties show that only the ligaments significantly affect head motion (Figure 5). Hence, mechanical properties of ligaments are critical in determining the severity of neck injuries.

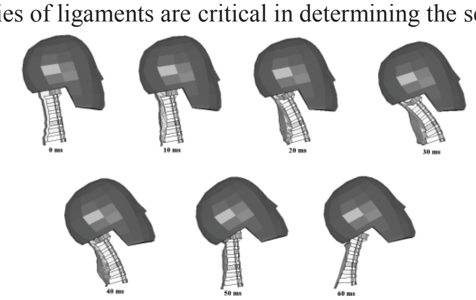

Figure 3: Head and neck motion during simulations.

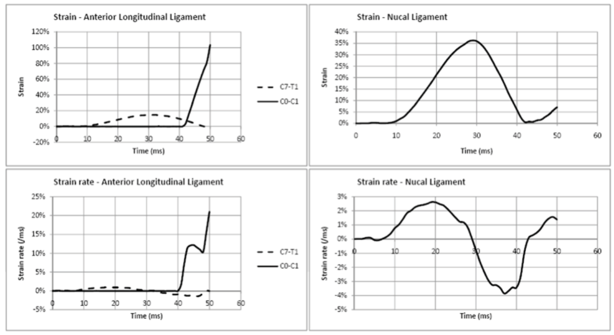

Figure 4: Strains and strain-rates experienced by ligaments.

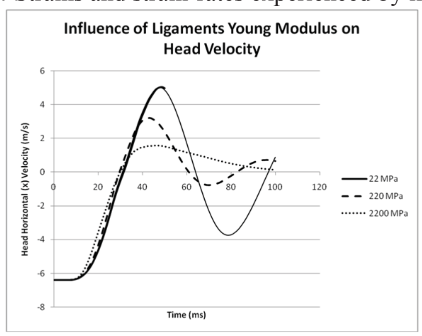

Figure 5: Influence of ligament mechanical properties on head motion.

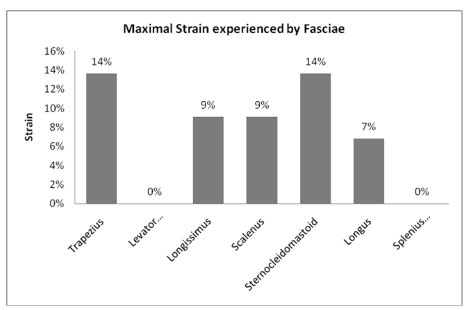

Figure 6: Maximal strain experienced by fasciae

Simulation results show that soft connective tissues experienced important strain rates. The higher portion (C0-C1) of the anterior longitudinal ligament experiences a strain-rate of 200 s^{-1} over the entire inter-vertebral region. The nuchal ligament reaches up to 40 s^{-1} in the same region (C0-C1) over a relatively wide area. Fasciae also show important strain rates but more locally and over short period of time. While strain rates of levator scapulae and splenius capitis fasciae remain negligible, other muscle fasciae (trapezius, longissimus, scalenus, sternocleidomastoid and longus) reach as high as 100 to 200 s^{-1}.

4. DISCUSSION

The use of advanced human body anatomical models as a mean to specify injury criteria helps avoiding unnecessary conservatism. Anatomical models provide a significant advantage over mechanical models (typical for crashworthiness): they can be used in different impact scenarios and as such, they provide a means to establish more precise injury criteria. They can also help to identify injury mechanisms that may vary depending on the kinematics of the impact (cf. Lau and Viano 1986).

For example, our study was conducted in order to figure out how to protect vehicle occupants against side blasts, given that occupants usually sit in a transverse direction. Results from our study

show that maximal strains are generally in the order of 15% to 35% for the anterior ligament at the different spinal levels (except at the higher extremity where it shows more than 100% and is more likely to rupture), similar to those reported by Ivancic et al. (2004) [56] who used a whole cervical spine mechanical model for studying whiplash. The new insight that emerges from our simulations is that head hyperextension follows a rebound from a hyperflexion of the neck, assuming that the nuchal ligament can sustain the load. In any case, failure of the nuchal ligament or the anterior longitudinal ligament in the C0-C1 region may lead to C0-C1 dislocation, an undesired situation. Hence, the injury mechanism proposed here suggests that both head hyperextension and hyperflexion must be limited by protective devices to limit neck injuries.

Predicted strains and strain rates bring some discussions about mechanical properties which should be observed at these levels. Results from Snedeker et al. (2005) [57] on porcine and human kidney capsules, which show strain and strain rates close to our results (ultimate strains of about 25% at a 200 s-1 strain rate), are actually very interesting regarding the possibility of connective tissue glass transitions at such strain rates. They report an elastic modulus E2 drastically changing at a strain rate of 20 s-1. Alternative models that include glass transition phenomena could potentially explain their results. Further testing at various intermediate strain rate levels (10 to 1000 s-1) should be conducted, however, to make sure that glass transition phenomena occur or not in this particular region which, incidentally, is the strain rate region observed in our simulations.

The model that we propose made a first attempt at including connective tissue fascia in the muscle models to investigate whether the presence of fascia would result in muscles playing a more significant role in restraining neck motion. The fascial muscle, although highly simplified, did not show additional muscle influence on neck motion that was shown to be mainly associated with ligament action. A refined model with more realistic honeycomb type fascia structure (Kjaer 2004 [58]) and mechanical properties dependent on strain rate could, however, affect this conclusion. Results from our simulations indicate that soft tissue characterization should be conducted over a strain rate varying from quasi static to a maximum of 300 s^{-1} in blast event situations. Those levels are incidentally well below those tested in the muscle characterization studies conducted by Sligtenshorst et al. (2006) or Song et al. (2007). They are, however, coherent with rabbit chest compression data reported by Lau and Viano (1986), muscle tissue compression data measured by McElhaney (1966) or kidney capsules measurements by Snedeker et al. (2005).

Predicting strain rates with models using mechanical properties which are valid at these same strain rates is somehow an iterative solution process, given that models are used to determine test data they need in order to be themselves valid. A simplified model such as the one that we propose in this paper, with linear mechanical properties might be used as a starting point. Given that material properties increase with strain rate, a linear model necessarily ends up with strain rates that are maximally conservative. If soft tissues get further characterized over this strain rate range, model results would be recomputed with new tissue properties, which would most likely be within strain rates that occur in the updated model. Improvement in the anatomical models could be easily considered given recent advances in finite element studies of the human body (e.g Shirazi-Adl 2006 [59]). However, we do not expect major variations in the model outcome for the estimation of the maximum strain rate range that occur in blast events. Moreover, more complex models may require more complex tissue characterization studies.

In this paper, we only considered the kinematics at the neck. When considering whole body response to mine blasts, other injury mechanisms may be involved. Shock waves produced are transmitted through the skull/spine up to the brain structures and those may induce local strains that may rupture critical regions of the brain (Kato et al. 2007 [60]). In addition, large accelerations of skull segments or skull deformations might also induce complex internal detrimental stresses to brain structures (Moss et al. 2009 [61]). Those phenomena, although important, were not investigated in this paper, neither were injuries at the lungs or the heart which are known to be sites for injuries in impact tests (Eiband 1959) or blasts (Ramasamy et al. 2008).

Our study shows the importance of an adequate design for military vehicle seats to absorb shock and dynamic loadings. An excellent design needs to focus on protecting the occupants not only from an IED's attack, but also in the event of an accident and at lower impacts (lower amplitude, long duration). Advanced shock absorption product already exists in the market but each design/material has its limitation. For example, the widespread use of foams in the industry comes from their unique compressive stress-strain behavior. However, most foams under very high strain rate enter their densification regime and thus amplify shock wave overpressure. Recent investigations suggest the use of polymeric foam in multi-layer protection systems.

5. CONCLUSION

This paper introduced a simplified finite element anatomical model of the neck to evaluate soft tissue strain rates that occur in the neck of light armour vehicle occupants exposed to side blasts. Results show that major soft tissue strains occur in the anterior longitudinal ligament during a neck hyperextension if a prior hyperextension-hyperflexion motion is made possible by the neck soft tissues i.e. if no tissue failure occurs beforehand. Our study suggests that neck failure occurs in the nuchal and/or anterior ligament at C0-C1 level such that the design of protective devices should therefore focus on limiting both head extension and flexion to avoid excessive rotation in that vertebral segment. Soft tissues sustain very high strain rate, in the range of 200 s-1 or 20 000 %/s. Such levels indicate the need to include more realistic soft tissue strain rate dependent tensile properties, including material failure thresholds in tension, for up to 300 s^{-1}. Although the model was based on linear material properties, results would not change significantly with more advanced anatomical models of the neck. Fasciae were included in a new muscle model, but despite this more accurate approach to modelling muscles, simulations show that protecting individuals by pre-contracting neck muscles is probably not an interesting approach to help limit neck injuries as the response is dominated by neck ligaments response.

Acknowledgements

This research project was funded in part by the Defense Research and Development Canada - Valcartier, as well as the National Sciences and Engineering Research Council of Canada.

References

[1] Eiband AM. 1959. Human tolerance to rapidly applied accelerations: a summary of the literature. NASA Memorandum. 5-19-59E, 94 p.
[2] Huculak P. 1990. A review of research and development in crash-worthiness of general aviation aircraft: seats, restraints and floor structures. National Research Council of Canada Aeronautical note NAE_AN-64, NRC Report No.: 31334.
[3] Stapp JP. 1961. Human Tolerance to Severe, Abrupt Deceleration, in Gravitational Stress in Aerospace Medicine. ed. by Gauer, O.H. and Zuidema, G.D. Little Brown and Co., Boston. pp 165- 188.
[4] Zaborowski AV, Rothstem JD, Brown WK. 1965. Investigations in Human Tolerance to Lateral Impact. 36th Annual Meeting, Aerospace Medical Association. April 1965. New York.
[5] Desjardins SP, Harrison H. 1972. The Design, Fabrication, and Testing of an Integrally Armored Crashworthy Crewseat. Dynamic Science, Division of Marshall Industries. U. S. Army Air Mobility Research and Development Laboratory, Fort Eustis, Virginia. Technical Report No.: 71-54. AD 742733.
[6] Gadd CW. 1962. Criteria for Injury Potential in Impact Acceleration Stress. NAS-NRC. Publication 977:141-145.
[7] Lowenhielm, P. 1975. Mathematical Simulation of Gliding Contusions. J Biomechanics. 8:351-356.
[8] Newman JA. 1986. A Generalized Model for Brain Injury Threshold (GAMBIT). International Conference on the Biomechanics of Impact (IRCOBI).
[9] Newman JA, Schewchenko N, Welbourne E. 2000. A proposed new biomechanical head injury assessment function - The Maximum power index, SAE Technical paper 2000-01-SC16.
[10] Digges KH. 1998. Injury Measurements and Criteria. Proceedings of RTO HFM specialists' meeting on Models for Aircrew Safety Assessment: Uses, Limitations and Requirements. RTO MP-20.
[11] Viano DC. 1984. Chest: Anatomy, Types and Mechanisms of Injury. Tolerance Criteria and LImits, and Injury Factors. General Motors Research Publication No. 4710.
[12] Eppinger RH. 1976. Prediction of Thoracic Injury Using Measureable Experimental Parameters, Report on the 6th International Technical Conference on Experimental Safety Verhicles, sponsored by the U.S. Department of Transportation, Washington D.C.. October 12-15.
[13] Lau IV, Viano DC. 1986. The viscous criterion - Bases and Applications of an Injury Severity Index for Soft Tissues. SAE Technical Paper 861882:123 -126.
[14] Lissner HR, Lebow M, Evans FG. 1960. Experimental Studies on the Relation Between Acceleration and Intracranial Pressure Changes. Man Surg Gyn and Obst III. pp. 329-338.

[15] King AI, Levine RS, Cheng R, Nakhla SS, Yang KH. 1981. Modelling of Human Surrogate Response to -Gx Impact Acceleration. Head and Neck Injury Criteria - A Consensus Workshop; Washington DC, March 26-27; US Department of Transportation. pp. 148-156.
[16] Stech EL, Payne PR. 1969. Dynamic Models of the Human Body. AMRL Technical Report 66-157, November 1969.
[17] Shane, S.J. 1985. Design and Testing of an Energy-Absorbing Crewseat for the F/FB- 111 Aircraft, Vol. 1 - Final Report, NASA CR 3916. August 1985.
[18] Coltman JW. 1983. Design and Test Criteria for Increased Energy-Absorbing Seat Effectiveness. US Department of Transportation, Federal Aviation Administration. Report No. FAA-AM-83-3.
[19] Chandler RF. 1985. Data for the Development of Criteria for General Aviation Seat and Restraint System Performance. SAE Paper 850851.
[20] King AI, Yang KH, Hardy WN. 2011. Recent firsts in cadaveric impact biomechanics research. Clinical Anatomy. 24:294-308.
[21] Stalnaker RL, McElhaney JH, Roberts VL. 1971. MSC Tolerance Curve for Human Head Impacts. Proceedings ASME Biomechanics of Human Factors Conference.
[22] Hannon P, Knapp K. 2006. Forensic Biomechanics. Lawyers & Judges Publishing Company Inc.
[23] Cheng H, Rizer AL, Obergefel LA. 1998. Generator of Body Data (GEBOD), Manual.
[24] Lockhart, P. 2010. Primary Blast Injury of the Head: Numerical Prediction and Evaluation of Protection. Master's thesis, University of Waterloo.
[25] Cheng H, Rizer AL, Obergefel LA. 1998. Articulated Total Body Model Version V - User's Manual. United States Air Force Laboratory. Report No.:AFRL-HE-TR-1998-0015.
[26] Sligtenhorst CV, Cronin, DS, Brodland, GW. 2006. High strain rate compressive properties of bovine muscle tissue determined using a split Hopkinson bar apparatus. J Biomechanics. 39:1852-1858.
[27] Song B, Chen W, Ge Y, Weerasooriya T. 2007. Dynamic and quasi-static compression response of porcine muscle. J Biomechanics. 40:2999-3005.
[28] McElhaney JH. 1966. Dynamic response of bone and muscle tissue. J Appl Physiol. 21(4):1231-1236.
[29] Zhang J, Song, B, Pintar, F, Yoganandan N, Chen W, Gennarelli TA. 2008. How to test brain and brain simulant at ballistic and blast strain rates. Rocky Mountain Bioengineering Symposium & International ISA Biomedical Sciences Instrumentation Symposium, Copper Mountain, Colorado, April 2008.
[30] Tanaka T. 1992. Phase Transitions of gels. Polyelectrolyte gels: Harland et al. American Chemical Society; Chapter 1; Washington, DC.
[31] Fathima NN, Baias M, Blumich B, Ramasami T. 2010. Structure and dynamics of water in native and tanned collagen fibers: Effect, of crosslinking. International Journal of Biological Macromolecules. 47:590-596.
[32] Tzou DL, Lee SM, Yeung HN. 1997. Temperature dependence and phase transition of proton relaxation of hydrated collagen in intact beef tendon via cross-relaxation spectroscopy. Mag Res Med. 37(3):359-365.
[33] Seiler T, Müller-Stolzenburg N, Wollensak J. 1983. Phase transitions in ocular tissue - NMR and temperature measurements. Graefe's Arch Clin Exp Ophtalmol. 21:122-125.
[34] Lillie MA, Gosline JM. 2002. The viscoelastic basis for the tensile strength of elastin, Int J Biol Macromolecules. 30:119-127.
[35] Ramasamy A, Harrisson SE, Clasper JC, Stewart MPM. 2008. Injuries from roadside improvised explosive devices. J Trauma Injury Infection and Critical Care. pp. 910-914.
[36] Linder A. 2000. A new mathematical neck model for a low-velocity rear-end impact dummy: evaluation of components influencing head kinematics. Accident Analysis and Prevention. 32:261-269.
[37] Küçük H. 2007. Biomechanical analysis of cervical spine sagittal stiffness characteristics. Comput Biol Med. 37:1283-1291.
[38] Jiango Z, Fang W, Qiang X, Haiyan S, Jun L. 2009. Development of a human neck finite element model. Second International Conference on Biomedical Engineering and Informatics, Tianjin, Oct 2009, pp.1-4.
[39] Bourdet N, Willinger R., 2008. Coupled head-neck-torso and seat model for car seat optimization under rear-end impact. Journal of Sound and Vibration. 313:891-907.

[40] Wittek A, Kajzer J, Haug E, Ono K. 2001. Finite element modelling of the muscle effects on kinematic responses of head-neck complex in frontal impact at high speed. JSME International Journal Series C. 44:2, 379-388.

[41] Van Lopik DW, Acar M. 2004. A computational model of the human head and neck system for the analysis of whiplash motion. International Journal of Crashworthiness. 9(5):465-473.

[42] Teo E, Zhang Q, Huang R. 2007. Finite element analysis of head-neck kinematics during motor vehicle accidents: Analysis in multiple planes. Medical Engineering & Physic. 29:54-60.

[43] Panzer M, Fice J, Cronin D. 2011. Cervical spine response in frontal crash. Medical Engineering & Physics. 33:1147-1159.

[44] McMinn RMH, Hutchings RT, Pegington J, Abrahams P. 1993. Color Atlas of Human Anatomy, Third Edition., Mosby – Year Book, Inc.

[45] Stemper BD, Yoganandan N, Pintar FA, Rao RD. 2006. Anterior longitudinal ligament injuries in whiplash may lead to cervical instability. Medical Engineering & Physics. 28:515-524.

[46] Conley MS, Stone MH, Nimmons M, Dudley GA. 1997. Specificity of resistance training responses in neck muscle size and strength. European Journal of Applied Physiology. 75:443-448.

[47] Kureshi A, Vaiude P, Nazhat SN, Petrie A, Brown RA. 2008. Matrix mechanical properties of transversalis fascia in inguinal herniation as a model for tissue expansion. Journal of Biomechanics. 41:3462-3468.

[48] Zeng YJ, Sun XP, Yang J, Wu WH, Xu XH, Yan YP. 2003. Mechanical properties of nasal fascia and periosteum. Clinical Biomechanics. 18:760-764.

[49] Haut TL, Haut RC. 1997. The state of tissue hydration determines the strain-rate-sensitive stiffness of human patellar tendon. J Biomechanics. 30:79-81.

[50] Panjabi MM, Crisco JJ, Lydon C, Dvorak J. 1998. The mechanical properties of human alar and transverse ligaments at slow and fast extension rates. Clinical Biomechanics. 13(2):112-120.

[51] Crisco JJ, Moore DC, McGovern RD. 2002. Strain-rate sensitivity of the rabbit MCL diminishes at traumatic loading rates. J Biomechanics. 35:1379-1385.

[52] Koh SW, Cavanaugh JM, Leach JP, Rouhana SW. 2004. Mechanical properties of the shoulder ligaments under quasi-static and dynamic loading. ISB XXth Congress – ASB 29th Annual Meeting. Cleveland, Ohio.

[53] Ng BH, Chou SM, Lim BH, Chong A. 2004. Strain rate effect on the failure properties of tendons. Proc Instn Mech. Engrs vol 218 Part H. Journal of Engineering in Medicine. pp. 203-206.

[54] Hukins DWL, Aspden RM, Hickey DS. 1990. Thoracolumbar fascia can increase the efficiency of the erector spinae muscles. Clinical Biomechanics. 5(1):30-34.

[55] Ward SR, Lieber RL, 2005. Density and hydration of fresh and fixed human skeletal muscle. J Biomechanics. 38(11):2317-2320.

[56] Ivancic PC, Pearson AM, Panjabi MM, Ito S. 2004. Injury of the anterior longitudinal ligament during whiplash simulation. European Spine Journal. 13:61-68.

[57] Snedeker JG, Niederer P, Schmidlin FR, Farshad M, Demetropoulos CK, Lee JB, Yang KH. 2005. Strain-rate dependent material properties of the porcine and human kidney capsule. J Biomechanics. 38:1011-1021.

[58] Kjaer M. 2004. Role of extracellular matrix in adaptation of tendon and skeletal muscle to mechanical loading. Physiological Review. 84:649-698.

[59] Shirazi-Adl A. 2006. Analysis of large compression loads on lumbar spine in flexion and in torsion using a novel wrapping element. J Biomechanics. 39:267-275.

[60] Kato K, Fujimura M, Nakagawa A, Saito A, Ohki T, Takayama K, Tominaga T. 2007. Pressure-dependent effect of shock waves on rat brain: induction of neuronal apoptosis mediated by a caspase-dependent pathway. J Neurosurg. 106(4):667-676.

[61] Moss WC, King MJ, Blackman EG. 2009. Skull flexure from blast waves: a mechanism for brain injury with implications for helmet design. Physical Rev Lett. 103(10):108702-1,4.